Bull Volcanol (2004) 66:322–335
DOI 10.1007/s00445-003-0313-y

RESEARCH ARTICLE

Nancy Riggs · Gerardo Carrasco-Nunez

Evolution of a complex isolated dome system, Cerro Pizarro, central México

Received: 16 August 2002 / Accepted: 23 July 2003 / Published online: 30 October 2003

Abstract Cerro Pizarro is an isolated rhyolitic dome in the intermontane Serdán-Oriental basin, located in the eastern Trans-Mexican Volcanic Belt. Cerro Pizarro erupted ~1.1 km^3 of magma at about 220 ka. Activity of Cerro Pizarro started with vent-clearing explosions at some depth; the resultant deposits contain clasts of local basement rocks, including Cretaceous limestone, ~0.46-Ma welded tuff, and basaltic lava. Subsequent explosive eruptions during earliest dome growth produced an alternating sequence of surge and fallout layers from an inferred small dome. As the dome grew both vertically and laterally, it developed an external glassy carapace due to rapid chilling. Instability of the dome during emplacement caused the partial gravitational collapse of its flanks producing various block-and-ash-flow deposits. After a brief period of repose, re-injection of magma caused formation of a cryptodome with pronounced deformation of the vitrophyric dome and the underlying units to orientations as steep as near vertical. This stage began apparently as a gas-poor eruption and no explosive phases accompanied the emplacement of the cryptodome. Soon after emplacement of the cryptodome, however, the western flank of the edifice catastrophically collapsed, causing a debris avalanche. A hiatus in eruptive activity was marked by erosion of the cone and emplacement of ignimbrite derived from a caldera to the north of Cerro Pizarro. The final growth of the dome growth produced its present shape; this growth was accompanied by multiple eruptions producing surge and fallout deposits that mantle the topography around Cerro Pizarro. The evolution of the Cerro Pizarro dome holds aspects in common with classic dome models and with larger stratovolcano systems. We suggest that models that predict a simple evolution for domes fail to account for possibilities in evolutionary paths. Specifically, the formation of a cryptodome in the early stages of dome formation may be far more common than generally recognized. Likewise, sector collapse of a dome, although apparently rare, is a potential hazard that must be recognized and for which planning must be done.

Keywords Dome · Cryptodome · Eastern Mexican Volcanic Belt · Dome collapse · Dome models

Editorial responsibility: J. Gilbert

N. Riggs (✉)
Department of Geology, Northern Arizona University,
Flagstaff, AZ 86011, USA
e-mail: nancy.riggs@nau.edu
Tel.: +1-928-5239362
Fax: +1-928-5239220

G. Carrasco-Nunez
Centro de Geociencias, Campus UNAM Juriquilla,
Apdo. Postal 1–742, 76001 Querétaro, Qro, Mexico

Introduction

Cryptodomes represent an unusual form of volcanic edifice in which a rising body of magma rises to a high level in the crust and actively deforms adjacent strata, but does not break through to the surface. Observations of cryptodome formation and eruption or destruction are very rare (i.e., Showa Shinzan: Ishikawa 1950; Minakami et al. 1951; Mount St. Helens: Moore and Albee 1981; Lipman et al. 1981). In some cases, a cryptodome will evolve to an extrusive feature that is then referred to as a dome (e.g., Mount St. Helens; Alid, Eritrea: Duffield et al. 1996; Mount Elden, Arizona, USA: Robinson 1913; Kluth and Kluth 1974), but the processes by which this happens are poorly documented. In addition, the question of why some upper crustal strata remain unaffected as dome magma intrudes, while in other cases country rock is deformed, remains unaddressed.

We describe here an intrusive and extrusive rhyolitic body with a complex evolution that involved several alternating stages of effusive and explosive activity. The forming dome went through evolutionary stages holding much in common not only with the cryptodomal activity of Showa Shinzan or Mount St. Helens, but in addition with collapsing stratovolcanoes and with small domes and dome complexes. Cerro Pizarro is a dome in the eastern Trans-Mexican Volcanic Belt, isolated from any large

magmatic system, that grew, erupted, partly collapsed, and regrew at ca. 220 ka. Our investigation of the volcano reveals both intrusive and extrusive stages that can provide a unique opportunity to clarify the pre-emergence processes that may accompany felsic dome eruptions. The evolution of Cerro Pizarro demonstrates that classic dome models may fail to account for a complex history of cryptodomal deformation that occurs in some cases before the magma body reaches the surface.

Regional geologic setting

The Trans-Mexican Volcanic Belt features broad volcanic fields and high-relief, nearly north–south-trending volcanic ranges separated by intermontane basins. Cerro Pizarro is located within the broad, internally drained Serdán-Oriental basin (Fig. 1), the easternmost intermontane basin of the Mexican High Plain (Altiplano).

The regional basement, composed mostly of Cretaceous limestone and some shale rocks, is exposed in a few isolated outcrops within the Serdán-Oriental basin. This basement was intruded in different places by relatively small plutons of granodioritic, monzonitic, and syenitic composition during Oligocene and Miocene times (Yáñez and García 1982). Volcanism has been on-going in the eastern Trans-Mexican Volcanic Belt since at least Miocene time (Yáñez-García 1982; Carrasco-Nuñez et al. 1997; Gómez-Tuena and Carrasco-Núñez 2000).

The Serdán-Oriental basin is a depression bounded to the east by the Citlaltépetl-Cofre de Perote chain (Fig. 1) of Quaternary andesitic stratovolcanoes, which forms a remarkable topographic divide that separates the High Plain from the Gulf of Mexico coastal plain. The chain apparently youngs southward, as the only active volcano is Citlaltépetl volcano (Pico de Orizaba) (Carrasco-Núñez 2000). To the south lies a range of highly folded and faulted Mesozoic sedimentary rocks. Northwestward is the Miocene andesitic Cerro Grande complex.

To the north, Los Humeros volcanic complex features a quasi-circular, ~20-km-diameter silicic caldera of Pleistocene age, which was responsible for a widespread distribution of voluminous pyroclastic deposits that now cover most of the Serdán-Oriental basin (Fig. 1). Two pyroclastic sheets derived from Los Humeros volcanic center are important in the history of Cerro Pizarro: the older, Xáltipan ignimbrite, is non-welded to partially welded and was erupted at ~0.46 Ma (Ferriz and Mahood 1984; Carrasco-Núñez et al. 1997). The younger, the Zaragoza ignimbrite, erupted at ~0.1 Ma. Basaltic lava flows to the east and west of Cerro Pizarro (Fig. 2) erupted from the older Los Humeros ring-fracture zone at less than 0.02 Ma (Ferriz and Mahood 1984); the magmatic system is still active as a geothermal field.

The Serdán-Oriental basin is characterized by monogenetic bimodal volcanism comprising (1) isolated but prominent rhyolitic domes (from north to south) Las Aguilas, Cerro Pizarro, Cerro Pinto, and Las Derrumbadas (Fig. 1), (2) relatively small, isolated cinder, scoria, and lava cones of basaltic composition that are only locally grouped to form small volcanic fields, and (3) explosion craters or maar structures including mostly tuff rings, some maars sensu strictu, and a few tuff cones.

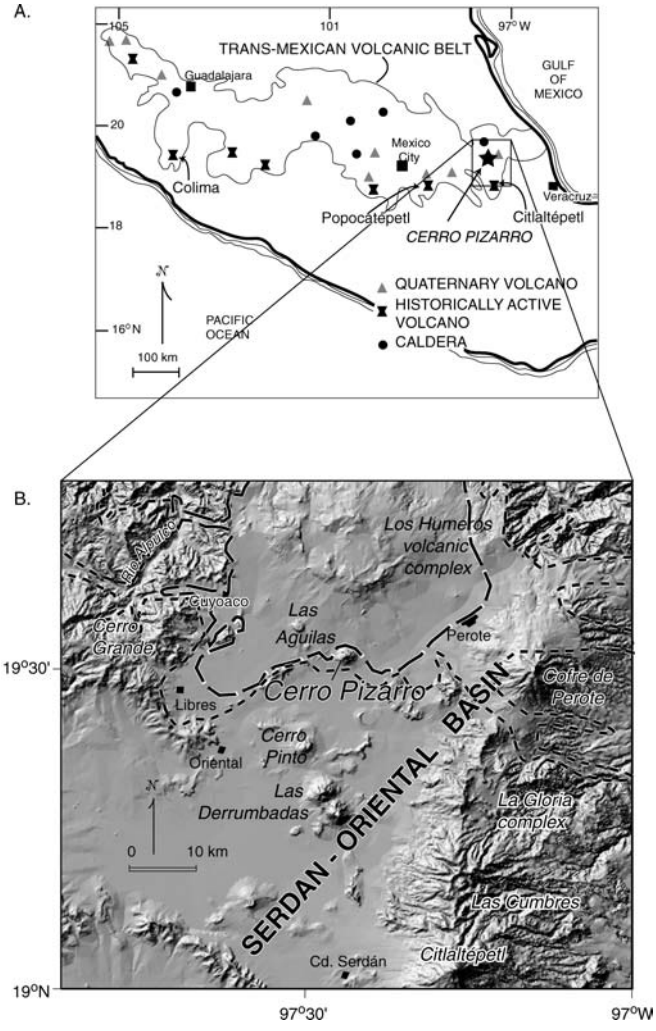

Fig. 1 **A** Central Mexico showing the Trans-Mexican Volcanic Belt. **B** DEM image of the Serdán Oriental basin in the eastern Trans-Mexican Volcanic Belt, showing Cerro Pizarro and other volcanoes of the eastern belt. *Short dashed line* represents likely outcrop areas of the Xáltipan ignimbrite prior to eruption of Cerro Pizarro; *long dashed line* represents outcrop areas of the Zaragoza ignimbrite; both derived from Los Humeros volcanic complex. Sierra Negra lies just to the south of the image area; La Malinche lies to the west

Cerro Pizarro dome

Cerro Pizarro is an isolated rhyolitic dome that lies near to both Citlaltépetl volcano and to Los Humeros volcanic center (Fig. 1), but was clearly not part of either system. $^{40}Ar/^{39}Ar$ dating of sanidine from a vitrophyre at Cerro Pizarro (New Mexico Geochronological Research Laboratory 2001) indicates an age of dome activity of 220,000±60,000 years, or middle Pleistocene. Strati-

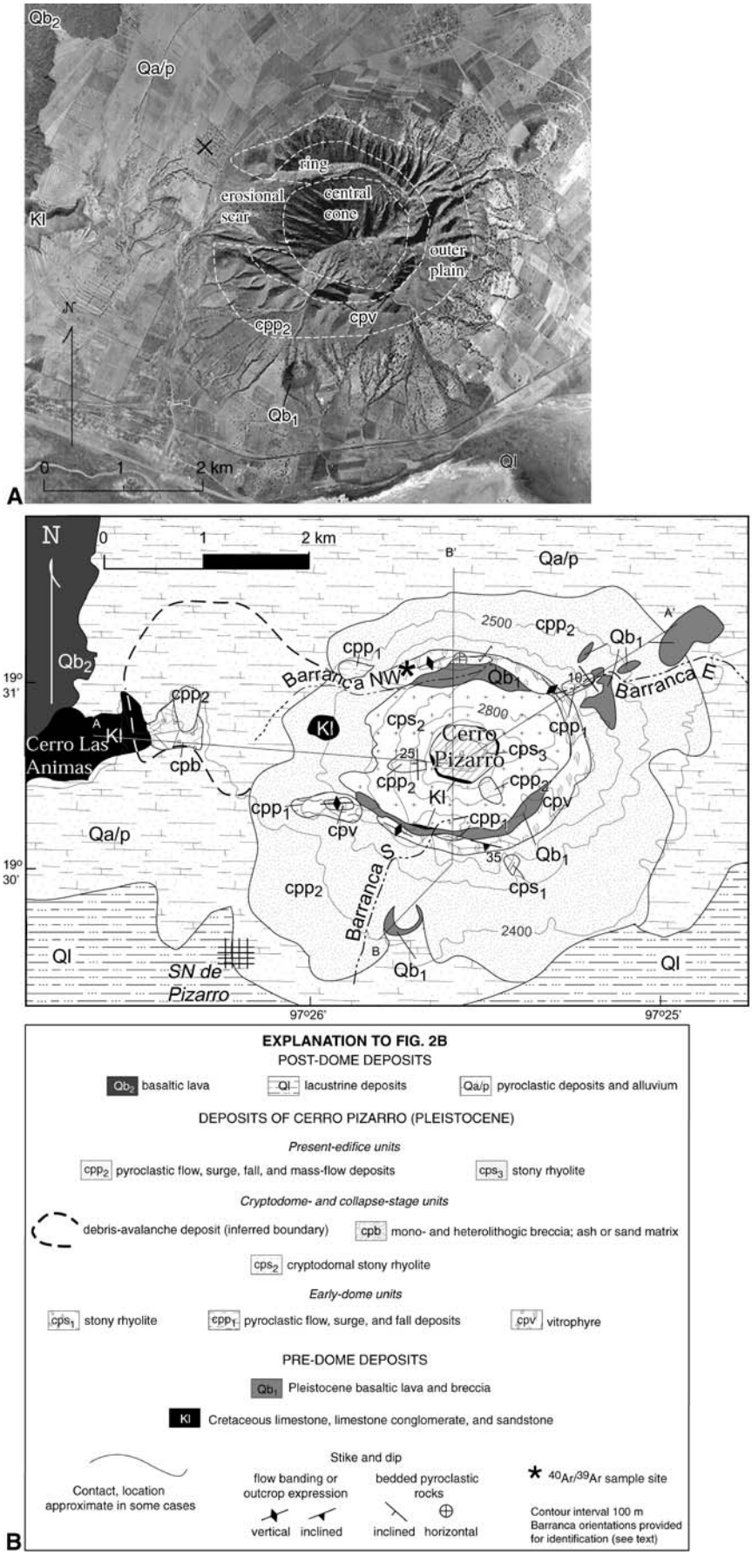

Fig. 2 A Aerial photograph and **B** geologic map of Cerro Pizarro. Contacts not drawn on photograph, but clear geologic features labeled (*letter symbols* as for Fig. 2B) for reference to geologic map

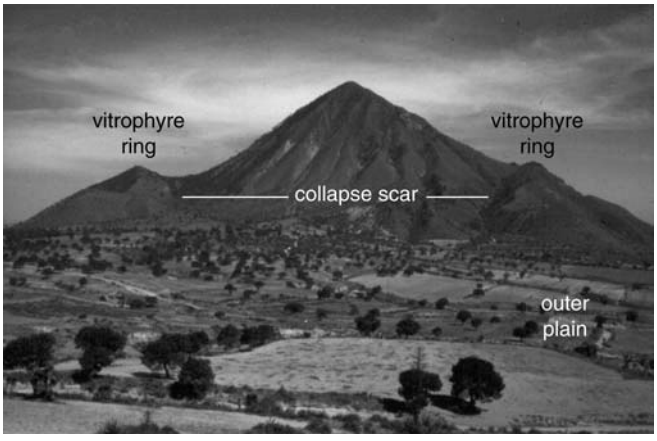

Fig. 3 View of Cerro Pizarro taken from Cerro Las Animas, approximately 3 km to the west (see Fig. 2B). Distinctive topographic shoulder half-way up the volcano marks the highest elevation of vitrophyre

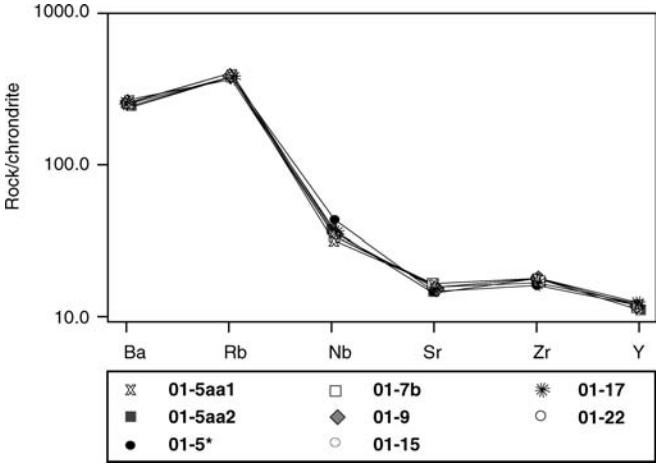

Fig. 4 Trace-element correlation diagram; values normalized to chrondrite. Sample numbers per Table 1

graphic evidence discussed below, however, casts some uncertainty on the total duration of dome activity.

Aerial photographs and geologic mapping of Cerro Pizarro reveal an approximately 2-km-wide, ~700-m-high edifice (Figs. 2 and 3). Small, older basaltic centers and deposits adjacent to Cerro Pizarro on several sides were not successfully dated, but stratigraphic evidence presented below indicates that at least locally they are similar in age to the dome. The cone is morphologically distinctive (Fig. 3): the central, conically shaped high area is surrounded by a resistant ring with a low broad apron surrounding the dome. The edifice is open to the west (Figs. 2A and 3) and moderately deeply incised elsewhere by canyons (referred to herein by the Spanish word, "barranca"). The climate of the Serdán-Oriental basin is semi-arid to arid, and whereas in the ~220 ka since emplacement most units have become moderately to strongly lithified, we infer that the overall shape of Cerro Pizarro has not been modified much by erosion. Interpretation of the morphology of the dome, together with an understanding of the facies, provides the basis for understanding its complex history.

Geochemical analysis of dome rocks indicates that the majority of erupted material contains 74–75%, SiO_2 and a very narrow range of trace-element concentrations (Table 1; Fig. 4). The rhyolite is weakly porphyritic, with less than 1% macroscopic sanidine, plagioclase, and quartz as much as 1.5 mm in diameter, and biotite generally no larger than 0.5 mm. The groundmass generally varies between variably highly to minorly glassy, with as much as ~25% microphenocrysts of feldspar and biotite to 0.1 mm.%

Generalized facies associations of Cerro Pizarro

Cerro Pizarro dome comprises two major facies associations, the massive lava dome and the volcaniclastic apron. Each association is repeated stratigraphically and is in various structural positions due to the complex history of the dome. In addition, pre-dome deposits make up a minor facies association.

Massive lava

Massive lava comprises stony rhyolite lava ($cps_{1, 2, 3}$, Fig. 2B) and vitrophyre (cpv, Fig. 2B). The stony lava is rich in microphenocrysts compared to vitrophyre, and gray to white, compared to black. Aside from these differences, the two are very similar in chemistry and mineral content and percentages (Table 1, Fig. 4). Flow banding is common in some areas, but is not pervasive. Pumiceous phases occur rarely in the vitrophyre or vitrophyric material, and exposures of breccia commonly found as carapace on rhyolite flows and domes are uncommon.

Volcaniclastic apron

The volcaniclastic-apron facies association includes all units deposited around the rhyolite lava core of the complex, and comprises coarse- and fine-grained deposits ($cpp_{1,2}$, cpb, Fig. 2B). Except where noted, all rhyolitic apron material is assumed to be derived from Cerro Pizarro, based on the proximity of the deposits, the similarity of their clasts to what is clearly dome material, and the lack of other sources close enough to Cerro Pizarro to provide the distribution of material found.

Coarse-grained deposits are divided into monolithologic, stony-rhyolite or stony-rhyolite with minor pumice breccia, and polylithologic breccia. Monolithologic in this case refers to the inference that both stony-rhyolite and pumice clasts were derived from the Cerro Pizarro dome. Breccia is clast supported and massive with commonly angular clasts from several mm to as much as 1 m in

Table 1 Geochemical analyses of Cerro Pizarro units, done by XRF on a Siemens 3000. Analytical procedures for major elements are described in Lozano-Santa Cruz et al. (1995). Analytical procedures for minor elements after Rosales-Hoz et al. (1997)

Element	Rel. SD (%)	01–5aa1[a]	01–5aa2[b]	01–5*[c]	01–7b[d]	01–9[e]	01–15[f]	01–17[g]	01–22[h]
SiO_2 (wt%)	0.7	75.31	73.88	73.91	74.65	74.11	74.81	75.35	74.53
TiO_2 (wt%)	6.3	0.09	0.09	0.09	0.09	0.10	0.09	0.10	0.09
Al_2O_3 (wt%)	0.7	13.75	13.62	13.79	13.75	14.21	13.62	13.72	13.59
Fe_2O_3 (wt%)	2.5	1.08	1.11	1.09	0.99	1.27	1.14	1.15	1.11
MnO (wt%)	11	0.06	0.06	0.06	0.06	0.06	0.06	0.06	0.06
MgO (wt%)	16	0.03	0.04	0.03	0.02	0.03	0.04	0.05	0.02
CaO (wt%)	3.6	0.85	0.77	0.79	0.78	1.01	0.85	0.86	0.78
Na_2O (wt%)	2.1	3.68	3.78	3.731	3.81	3.90	3.67	3.78	3.73
K_2O (wt%)	0.5	4.4	4.31	4.52	4.35	4.41	4.35	4.36	4.46
P_2O_5 (wt%)	10	0.04	0.05	0.04	0.05	0.10	0.05	0.04	0.05
LOI (wt%)	-	1.30	1.92	1.35	1.81	0.23	1.97	1.13	1.35
Total (%)		100.58	100.23	100.82	100.51	99.33	100.49	99.15	99.13
Rb (ppm)	5.7	133	131	133	129	131	128	129	132
Sr (ppm)	0.4	176	181	176	176	177	194	205	181
Ba (ppm)	3.2	1,726	1,718	1,773	1,703	1,658	1,721	1,772	1,776
Y (ppm)	2.4	23	23	24	24	23	23	23	23
Zr (ppm)	0.4	110	111	113	110	109	117	122	116
Nb (ppm)	6.3	13	13	15	13	13	11	13	12
V (ppm)	1.8	6	<5	<5	<5	<5	10	<5	8
Cr (ppm)	8.1	8	9	7	10	9	7	8	9
Co (ppm)	6.8	<3	<3	<3	<3	<3	<3	<3	<3
Ni (ppm)	3.6	<1	<1	<1	<1	<1	<1	<1	<1
Cu (ppm)	5.3	10	14	12	8	10	13	16	17
Zn (ppm)	1.9	49	48	45	44	40	46	45	43
Th (ppm)	-	<3	<3	<3	<3	<3	<3	<3	<3
Pb (ppm)	-	21	22	25	22	22	22	23	21

[a] 01–5aa1: Vitrophyre clast from debris-avalanche deposit; cpb at C. Las Animas (cpv clast)
[b] 01–5aa2: Banded stony rhyolite clast from debris-avalanche deposit; cpb at C. Las Animas (cps1 clast)
[c] 01–5*: Vitrophyre clast from debris-avalanche deposit; cpb at C. Las Animas (cpv clast)
[d] 01–7b: Vitrophyre from ring, south side of volcano; cpv
[e] 01–9: Banded stony rhyolite from south flank of cone; cps3
[f] 01–15: Stony rhyolite from cpp1 in outer plain, west side of volcano; cps2
[g] 01–17: Vitrophyric rhyolite from ring, southwestern side of volcano; cpv
[h] 01–22: Vitrophyric rhyolite from ring, east side of volcano; cpv

diameter in a matrix of fine to coarse ash. Sorting is poor and deposits are as much as 20 m thick.

Polylithologic breccia contains both volcanic clasts and underlying, pre-volcanic rock types. Clasts are generally 1 cm to as much as 3 m in diameter and round to angular and comprise any combination of stony rhyolite, vitrophyre, basement limestone, highly weathered and altered basalt, unaltered basalt, and/or Xáltipan ignimbrite. Deposits are generally poorly sorted and are as much as 5 m thick. Beds are structureless to faintly bedded. Matrix supports the clasts and is comminuted stony rhyolite, ash, and/or quartz and feldspar sand grains.

Fine-grained deposits are well sorted and planar, and are composed of pumice and ash or of pumice and ash mixed with lithic clasts. Cross bedding and normal or reverse grading are locally common. Clast sizes vary from 2–50 mm and consist of stony or vitrophyric rhyolite or basalt; individual beds are 2–3 cm to as much as 10 cm thick.

Volcaniclastic rocks, whether fine or coarse grained, are further divided by composition into two primary groups, those with vitrophyre clasts and those without. As explained below, this distinction, together, in some cases, with stratigraphic position, allows us to determine where units belong in the overall stratigraphy of the cone.

Pre-dome deposits

Rhyolitic lava and volcaniclastic rocks associated with Cerro Pizarro were emplaced onto a landscape that was apparently dotted by exposures of basement limestone, Xáltipan ignimbrite derived from the Los Humeros volcanic complex, and small basaltic scoria cones. Limestone conglomerate, which contains rounded clasts up to approximately 35 cm in a matrix of fine limestone and quartz grains, is spatially intermixed with massive-lava facies association rocks. Rounded limestone clasts also occur in some apron facies-association breccias. Xáltipan ignimbrite occurs primarily as clasts in apron facies-association deposits. Basaltic scoria-cone deposits comprise structureless lava, flow breccia, basaltic ash-flow tuff, and scoria beds. In some places, for example east of Barranca S near its southern terminus (Fig. 2B), the original shape of the scoria cone is apparent and beds of scoria are well preserved. Elsewhere, for example in the upper reaches of Barranca S, scoria, flow breccia, and lava are intermixed and do not present a coherent assemblage of rocks.

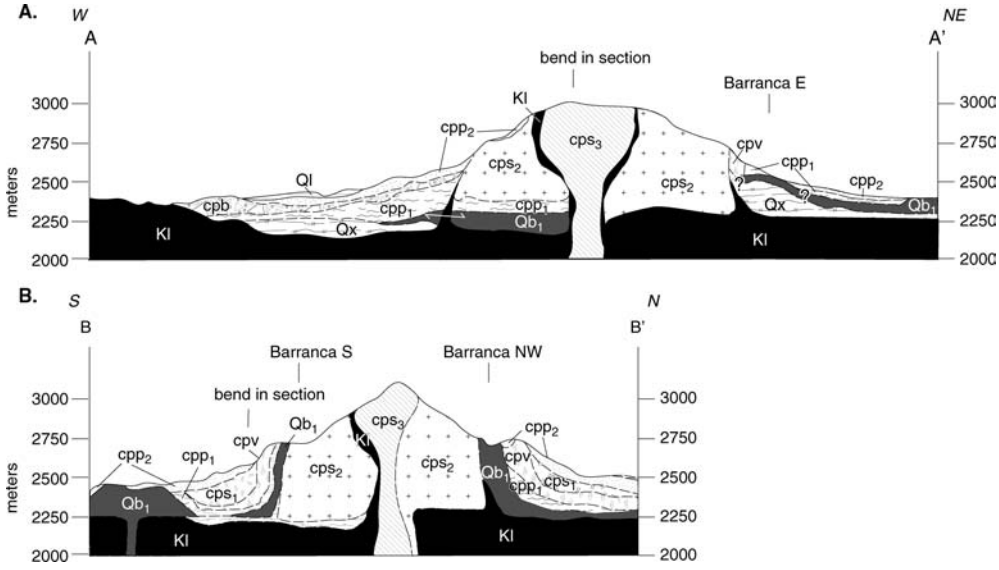

Fig. 5 Cross sections approximately east–west (**A**) and north–south (**B**) through Cerro Pizarro. For locations see Fig. 2B. *Symbols* as for Fig. 2B, with the addition of Qx, Quaternary Xáltipan ignimbrite

Stratigraphy of Cerro Pizarro

The geology of Cerro Pizarro is highly heterogeneous around the cone, but a synthesis of the facies present, together with the structure of the complex, provides a basis for understanding the evolution of the system. Here, we present short descriptions of sections around the volcano, without attempting to describe the distribution of specific units in detail.

The rocks exposed in Barranca E (Fig. 2B) represent the volcaniclastic-apron and pre-dome facies associations. The stratigraphic section has flat-lying basaltic ash-flow tuff and breccia (Qb_1, Figs. 2A and 5A) at its base, overlain by pyroclastic strata (cpp_1, Fig. 2B; Fig. 5A). The pyroclastic rocks, which crop out in a section as much as 15 m thick, comprise thin- to thick-bedded, well-sorted, planar to cross-bedded rhyolitic pumice and ash. Clasts in the lower, pumice-and-ash section are stony rhyolite with minor basalt and are less than 1–2 cm in diameter. This succession is overlain by a breccia with an ash matrix; at the base of the breccia, blocks are completely encased by ash and pumice of the underlying unit (Fig. 6). Blocks are up to 100 cm in diameter and also consist solely of stony rhyolite. The breccia is in complex contact with vitrophyre (cpv, Figs. 2B and 5A): the contact itself is not exposed, but mapping relations suggest that within approximately 50 m orientations change from nearly flat lying in the pyroclastic strata to nearly vertical in the vitrophyre (Fig. 5A). Breccia is poorly exposed in this 50-m section, and its orientation is unclear.

Sections on either side of Barranca NW expose different massive-lava, apron, and pre-dome facies-associations rocks. Both sides contain a pyroclastic succession (cpp_2) that comprises dominantly well-sorted pumice-pebble conglomerate overlain by fine-grained ash and pumice-grain beds that are plane and cross-bedded. Vitrophyre fragments are common throughout. On the north side of the canyon, the basal pumice conglomerate overlies massive vitrophyre and vitrophyre blocks (cpv); on the south side pumice conglomerate overlies basaltic lava and scoria (Qb_1), and basalt is a common clast type in the lowest pumice deposits. At the mouth of the canyon, ash-matrix breccia contains a highly diverse clast assemblage of basalt, vitrophyre, stony rhyolite, and rare Xáltipan ignimbrite.

Fig. 6 Pyroclastic succession in Barranca E. Intermixing of bedded pyroclastic deposits and blocks at base of block-and-ash-flow deposit indicates that dome collapse began as explosive eruptions were waning but still ongoing. Scale marked in 1-cm intervals

Barranca S contains a stratigraphic section that dips as much as 90° and includes massive-lava, apron, and pre-dome facies-associations rocks (Fig. 5B). Due to post-depositional deformation, original stratigraphic thicknesses are not preserved. From south to north, the section comprises vitrophyre (cpv), finely bedded, well-sorted pyroclastic strata (cpp_1), limestone- and Xáltipan-clast breccia (included in cpp_1), and basaltic lava and scoria (Qb_1). The breccia consists of sub-rounded to subangular clasts of Xáltipan ignimbrite, altered basalt, limestone,

Fig. 7 Basaltic rocks (*dark*) in complex contact with rhyolitic pyroclastic material (*light*) derived from Cerro Pizarro. Interleaved, structureless units suggest that the basaltic strata were not coherent consolidated material when disruption of both units occurred. Hammer head is ~20 cm long

and other unidentified rhyolitic volcanic material in an ash matrix. This deposit is poorly exposed both here and in scattered outcrops elsewhere around the dome, and internal structures and the total thickness of the unit are not preserved. Limestone clasts are the largest and are up to 20 cm in diameter. The pyroclastic strata comprise very fine ash with granules of pumice and rare outsize basaltic clasts as much as 30 cm in diameter. Layers of basaltic and stony rhyolite pebbles to 2 cm are interbedded with ash-rich layers; vitrophyre is not present as a clast type anywhere in this pyroclastic succession. North of the basalt, apparently flat-lying pyroclastic material is rich in stony rhyolite but not vitrophyre; the contact between this pyroclastic material and either basalt or dome material is not exposed. Along the ridge at the head of Barranca S, basalt is chaotically intermixed with pyroclastic material (Fig. 7). Bedding in the pyroclastic material is destroyed and the basalt consists of fragments of scoria and lava as much as 1.5 m in diameter. Contacts are contorted and irregular.

Exposures in some areas high on the dome consist of a succession approximately 25 m thick and laterally extensive over several tens of meters (Figs. 2B, 5). The succession is highly contorted or vertically dipping. Limestone conglomerate and sandstone (Kl) are ~5 m thick. The conglomerate is in contact with approximately 3 m of rhyolitic pyroclastic strata and a breccia ~3 m thick that contains ash and blocks of stony rhyolite to approximately 30 cm. This pyroclastic succession yields uphill to altered, flow-banded, stony-rhyolite breccia. Clasts range in size from 2 cm to 2+ m, and are cemented by an orange, highly altered matrix. Succeeding this entire succession is faintly flow-banded rhyolite (cps_3) that is in continuous exposure to the top of the volcano.

The area west of Cerro Pizarro, called here the Cerro Las Animas section, contains only volcaniclastic-apron facies association strata. Here, massive monolithologic breccia deposits (cpb) are chaotically intermixed. Monolithologic breccia consists of clasts of either stony or vitrophyric rhyolite, and clasts are as much as 2.5 m in diameter. Stony rhyolite clasts often display jigsaw fracturing. Breccia is clast supported with an ashy matrix. Contacts between breccia deposits are very rarely exposed and consist of altered finely comminuted rhyolite and possibly ash. Polylithologic breccia (cpb), which overlies the monolithologic breccia everywhere, contains clasts of Xáltipan ignimbrite, altered and unaltered basalt, stony rhyolite, and vitrophyre. In outcrop these clasts are generally less than ~20 cm and sub-rounded, but in float boulders as much as 3 m in diameter of Xáltipan ignimbrite and other volcanic rocks are not uncommon. Locally this breccia is faintly stratified.

Original size and potentially characteristic shapes of breccia deposits (e.g., hummocks) are lacking. Post-eruptive reworking, together with emplacement of later deposits, have eroded and/or buried original outcrops.

Morphology of the dome

Much of the understanding of Cerro Pizarro derives from an interpretation of the its morphology. The complex is divided into a central cone area, its surrounding ring, the outer plain, and the west-facing erosional scar and related features (Fig. 2A).

The central area comprises dominantly massive stony rhyolite. It is conical in shape (Fig. 3), which probably approximately reflects the original shape of the cryptodome body. Limestone conglomerate and pyroclastic deposits high on the slopes of Cerro Pizarro (Fig. 2B) are in contact with stony rhyolite above and below structurally. Vitrophyre is absent from this area.

The ring that surrounds the central cone area is made up of rocks dominantly of the massive-lava and pre-dome facies associations. Rocks dip from approximately 35° away from the cone to vertical, but, as described above, stratigraphic successions are locally intact. The variable resistance of various units gives a distinct shape to the ring (Fig. 3): an eroded tuff bed between the central cone and resistant vitrophyre in the ring causes lower topography that gives the general aspect of a moat.

The continuity of the ring is broken in two major locations. In one place, along the southern margin of Cerro Pizarro, a major canyon disrupts essentially continuous bedding around the cone (i.e., on both sides of the canyon, bedding is steep to vertical). The other, discussed more fully below, is on the west side of the cone.

The outer plain of Cerro Pizarro comprises gently dipping to flat-lying strata that represent dominantly apron and pre-dome facies associations. Minor stony rhyolite is present. Units include pyroclastic breccia and fine-grained rocks, basaltic scoria-cone deposits, and limestone conglomerate. In rare cases, units can be traced outward from steeply dipping ring exposures to flat-lying outcrops on the outer plain.

The west side of Cerro Pizarro is marked by a topographic discontinuity in the inner ring. On an aerial photograph (Fig. 2A), this discontinuity is horseshoe shaped, and is strongly reminiscent of flank-collapse scars at certain large stratovolcanoes such as Mount St. Helens. To the south of this gap, beds in the ring strike approximately towards the west, contrasting with the more NW-SE strike of strata just to the north (foliation symbols, Fig. 2B). Two kilometers to the west of the cone, at Cerro Las Animas, Cerro Pizarro strata are juxtaposed against a ridge of Cretaceous limestone (Fig. 2B).

History and evolution of Cerro Pizarro

Early dome evolution

The oldest Cerro Pizarro-related stratum is breccia that contains only clasts of pre-Cerro Pizarro units (e.g., Barranca S, see above). Source limestone is exposed a minimum of 3 km from the breccia, and most other pre-Cerro Pizarro volcanic material are not presently exposed at the surface for several km. Due to the inclusion of what was likely buried material, we have interpreted this unit as an explosive breccia associated with the early phases of vent formation, similar to vent-expansion breccias often documented around domes (e.g., Christiansen and Lipman 1966; Duffield et al. 1995).

Pyroclastic deposits related to the earliest phases of dome development are preserved locally in the ring that surrounds the lava core, for example those in Barranca S (cpp_l, Figs. 2B and 5B). We interpret these strata as ash eruptions from the vent of a small dome that breached the surface, but that does not need to have been of great height (Fig. 8A). Sedimentary structures in these fine-grained deposits suggest that they were emplaced dominantly by fall processes, but pebble beds suggest that some water reworking may have occurred.

During or after explosive activity, a dome continued to form, potentially of a form commonly recognized in dome models (e.g., Christiansen and Lipman 1966; Duffield et al. 1995; Riggs et al. 1997). Evidence does not remain concerning the original form, but the dome was characterized by a carapace of massive and brecciated vitrophyre (Figs. 8B and 9). Deposits associated with eruption of the dome belong to the volcaniclastic-apron facies association, e.g., massive, clast-supported breccia and thick pyroclastic strata preserved in Barranca E. We interpret the clast-supported monolithologic breccias (cpp_l) in Barranca E and elsewhere around the dome as block-and-ash-flow deposits. The fact that these breccias lack vitrophyre suggests that either vitrophyre was developed irregularly around the dome, or that collapse of the dome occurred before the vitrophyre was fully formed. The intimate relation between the top of the 15-m-thick succession of fine beds and the base of the block-and-ash-flow breccia in Barranca E (Fig. 6) indicates that dome collapse began during the last stages of vertical eruption. In summary, the first phases of evolution involved dome formation, with episodes of partial collapse (Figs. 8A, B).

Cryptodome

Formation of the initial dome was followed by some period of relative quiescence. The similarity of mineralogy and chemistry of the various rhyolites in the complex (Table 1 and Fig. 4) suggests that this quiescence was brief, perhaps on the order of decades. Hildreth and Drake (1992) noted that lava and plinian material only 86 years different in age from Volcán Quizapo have nearly identical chemical signatures, whereas lava perhaps a few hundred years older has markedly different chemistry. Pyroclastic deposits specific to this time of quiescence are lacking at Cerro Pizarro.

Evidence for the next phase of activity derives from the ring, where strata are moderately dipping to vertical, but remain in stratigraphic order (Figs. 5 and 8C). This phase of magma emplacement was likely endogenous. Because overlying strata were bowed up we refer to this emplacement as a cryptodome (cf. Mount St. Helens, Moore and Albee 1981), but unlike other documented cryptodomes (Mount St Helens, Showa Shinzan: Minakami et al. 1951), the Cerro Pizarro cryptodome intruded and deformed coherent dome facies. Intruding magma bowed up pre-existing strata (Fig. 8C) to orientations that range from vertical to 30° (Fig. 2B); in some places, deformation was minor. Deformation of some pre-cryptodome stratigraphic units, together with apparent hydrothermal alteration and silicification, led to a strongly resistant "rib" of vitrophyre and basaltic units encircling a stony rhyolite core (Fig. 5). We speculate that hydrothermal fluids from the rising cryptodome caused alteration and weakening of the devitrified stony interior of the previously formed dome. Erosion of this altered material, in turn, may explain the present-day dip in topography between the vitrophyre/basalt ring and the massive interior core.

Use of the word cryptodome implies that a coherent "roof" remained over the intruding magma body. Evidence for this roof lies primarily in the irregular structural pattern of deformation and the effects on deformed rocks. In the former cases at Cerro Pizarro, as was documented at Showa Shinzan (Mimatsu 1995), overlying country rocks were not simply all raised to a uniform orientation. At Showa Shinzan the documented pattern shows irregular zones of near-vertical and near-horizontal deformation. Evidence for an irregular roof pattern only remains in the ring at Cerro Pizarro, but dips range from as low as 35° to vertical. The effects on deformed rocks are not *prime facie* evidence of a cryptodome roof, but are most easily explained by assuming that they were affected by rising terrain. Basaltic and pyroclastic material at Cerro Pizarro locally slumped and intermixed, suggesting that some amount of free space was available. This is more easily attributed to deformation over the roof of a rising

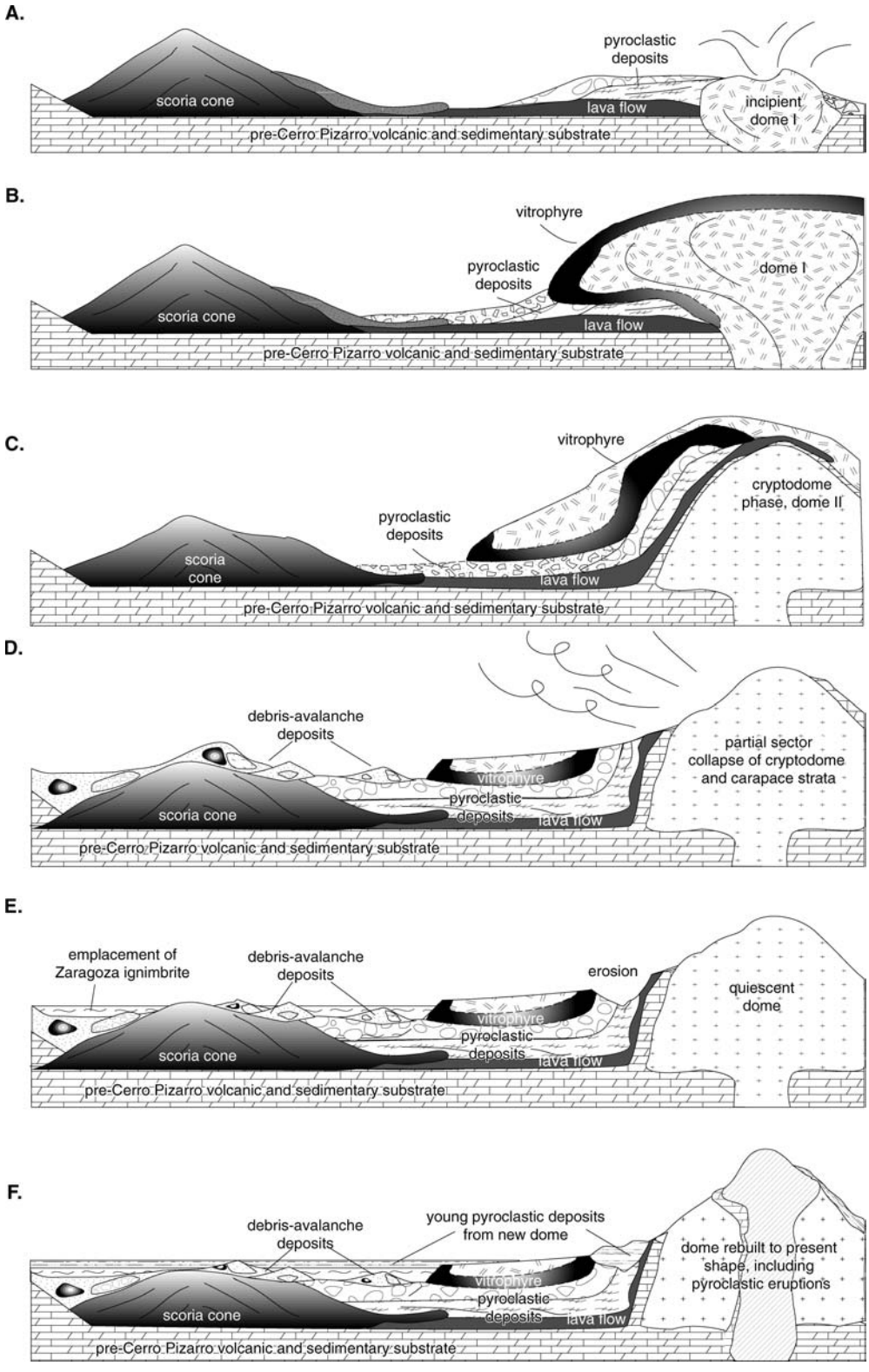

Fig. 8 Evolution of the Cerro Pizarro dome. **A** Earliest phase, during which incipient dome activity produces pyroclastic deposits and a "vent-clearing" breccia, both of which overlie older basaltic scoria-cone deposits. **B** Growth and eruption of coherent dome with vitrophyric carapace. **C** Intrusion of a cryptodome deforms country rock to vertical and near-vertical orientations. **D** Sector collapse of the cryptodome removes most of the intrusive material and all the extrusive material above ~ 2700 m, forming a debris avalanche. **E** Hiatus period, marked by erosion of dome and reworking of debris-avalanche deposit. **F** Intrusion and eruption of youngest cone-building material

magma body. Vitrophyre, in contrast, was dominantly highly coherent, forming near-vertical walls up to 75 m high. This contrast is presumably due to mechanical properties of the material. The presence of contorted and mixed basaltic and pyroclastic strata also supports the inference that the hiatuses between basaltic and rhyolitic volcanism, and between events that built the complex, were not long.

The outcrop pattern in the ring indicates that inflation of the cone due to emplacement of the cryptodome was

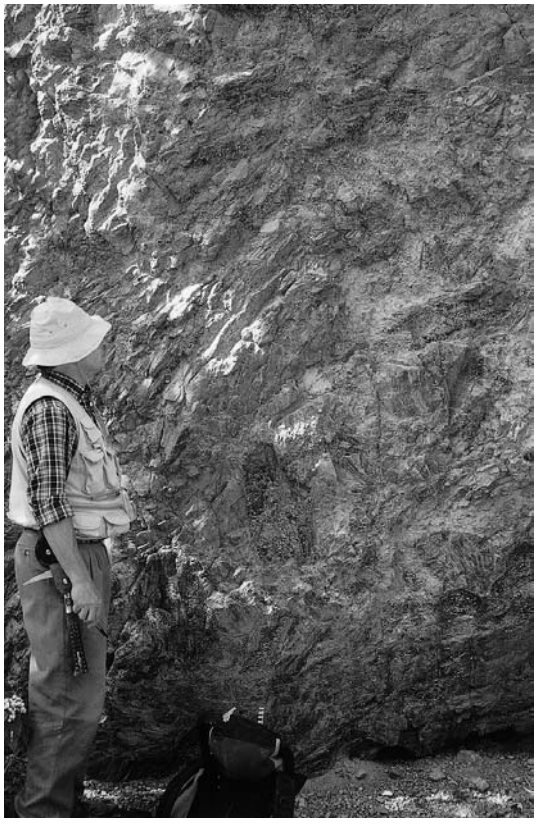

Fig. 9 Vitrophyre breccia on the south side of Cerro Pizarro. Although this outcrop is presently vertical, we infer that it represents original carapace on the early dome

highly irregular. The morphology of the remnant vitrophyre "rib" suggests that the center of intrusion was approximately central to the cone. Documentation of the shallow deformation associated with cryptodome emplacement at Mount St. Helens (Lipman et al. 1981) and likely deeper deformation at Alid volcano in Eritrea (Duffield et al. 1996 and personal communication 2002) suggests that deformation may often be uniform. The cryptodome at Showa Shinzan (Mimatsu 1995), in contrast, like that at Cerro Pizarro, deformed surficial materials in an irregular manner.

To assess the size of the dome at this point, we assume that the base elevation of the cone has stayed approximately constant over time. Based on the morphology of the ring and its elevation, we infer that at this time the volcano stood about 400 m high, compared to the present height of 700 m.

Sector collapse

Deposits that represent the evolution of Cerro Pizarro are generally confined to the immediate vicinity of the mountain. A major exception to this, however, are the chaotic mixed mono- and polylithologic breccia deposits that lie between two and approximately three km west of the cone, to the west of a major gap in the ring as described above. This gap, together with the chaotic nature of the breccia deposits to the west, strongly suggests that a portion of the cone was destroyed by collapse (Fig. 8D), in a manner similar to the partial destruction of Mount St. Helens, USA, in 1980 and Bezymianny, Kamchatka, in 1956 (Gorshkov 1959; Belousov 1996), but at smaller scale (Table 2). The breccia that abuts the ridge of Cretaceous limestone west of the ridge is interpreted as debris-avalanche deposit. The height/runout ratio, used by Ui (1983) and Siebert (1984) to distinguish debris avalanches from other kinds of mass flows, is ~0.2, or within the range suggested for this type of deposit (Fig. 10). The volume of material removed, approximately 0.3 km^3, is about half an order of magnitude larger than the collapses documented at Soufrière Hills (Sparks et al. 2002; Voight et al. 2002c; Table 2).

Ui et al. (2001) discuss mechanisms by which debris avalanches can be produced, ranging from phreatic eruption and/or disintegration of a hydrothermally weakened part of the volcano (Bandai, Japan, 1888; also Soufrière Hills, Sparks et al. 2002; Voight et al. 2002c), to intrusion of a new batch of magma and resultant

Table 2 Comparison of collapse volume, area covered by collapse deposits, and area of resultant scare for stratovolcano collapse (Mount St. Helens, Bezymianny, and Mt. Shasta) and dome complex or isolated dome (Soufrière Hills, Cerro Pizarro). Differences between the area covered by the collapse deposits is attributed largely to the topography and drainage system of the volcano

Volcano	Approximate volume of material removed from volcano	Area covered by blast and/or debris-avalanche deposits	Area of scar	Reference
Mount St. Helens	~2.76 km^3	~60 km^2	~2×4 km	Voight et al. (1981)
Bezymianny	~1 km^3	~550 km^2	~1.5×3 km	Gorshkov (1959); Belousov (1996)
Mt. Shasta	Unknown	>675 km^2	n/a	Crandell et al. (1984); Crandell (1989)
Soufrière Hills	0.08–0.09 km^3	~15 km^2	~0.4×0.5 km	Sparks et al. (2002); Voight et al. (2002c)
Cerro Pizarro	~0.3 km^3[a]	~5 km^2[a]	~1.25×1 km	This study

[a] Volume of removed material based on approximately symmetrical cone prior to collapse; area covered by debris-avalanche deposit based on present area underlain by these deposits plus inferred filled paleo-topography

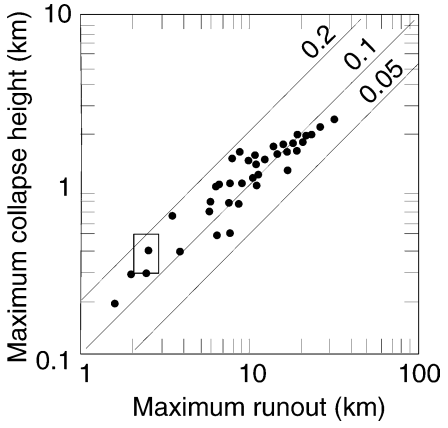

Fig. 10 Collapse height vs. runout distance for debris avalanches, after Ui et al. 2001. *Box* represents Cerro Pizarro; size of box reflects uncertainties in initial collapse height and likely final distance of runout

instability of the edifice (Mount St. Helens), or to earthquakes (Unzen, Japan, 1792). Voight et al. (2002c) also attribute collapse at Soufrière Hills to loading due to dome development and earthquake activity. Evidence for the causal mechanism of sector collapse at Cerro Pizarro is sparse: (1) ash matrix within monolithologic breccia at Cerro Las Animas (Fig. 2B); (2) the outcrop pattern of the vitrophyre rib on the west side of the cone, which opens out to the west (Fig. 2B), rather than rocks just being missing; (3) small-scale faults (<<1 m offset), which are common in some deposits around the cone. No other apparently related deposits, such as the blast surge found at Mount St. Helens (Fisher 1990), support the inference that active explosions were causal or even occurring. Likewise, altered clasts are extremely rare, suggesting that hydrothermal alteration was not prevalent in the cone.

Two causal mechanisms seem most likely. The first suggests that the rapid emplacement of fresh magma in the cryptodome, likely combined with a swarm of earthquakes, acted to destabilize a major portion of the cone to expose fresh magma. This may then have partially explosively erupted. The new magma must have concentrated in the western portion of the cone, and more intensive fracturing may have occurred there in response to cryptodomal stresses yielding collapse to the west. The morphology of the scar and the vitrophyre rib of the ring, however, suggest that the growth and locus of collapse were near the top of the cone present at that time. The second likely mechanism is Mount St. Helens-style explosive eruption. An erosional period followed the collapse (see below) and during this time blast deposits could easily have eroded; such deposits have a relatively low preservation potential in the geologic record. Evidence against explosive eruption, aside from the lack of clearly related pyroclastic deposits, is the remarkable coherence of the vitrophyre where it is still preserved around the cone: considering the relatively small size of the edifice, intense disruption of the vitrophyre might be expected during a violent explosion.

Also possible is a large-scale landslide, without influence of magma. A landslide would yield brecciated blocks as seen at Cerro Las Animas, but a landslide without associated explosive eruption would not likely have caused the vitrophyre rib to "bend" outward to the west, unless the vitrophyre was still ductile.

Hiatus

Following emplacement of the debris-avalanche deposit, a significant period of weathering and erosion ensued (Fig. 8E). Evidence for this period is multi-fold, including erosional features and stratigraphic relations.

The best evidence for erosion comes from Barranca NW (Fig. 2B), where young pyroclastic material (cpp_2) overlies vitrophyric or basaltic material. The mouth of the barranca exposes polylithologic breccia containing clasts of dense rhyolite, vitrophyre, and basalt. The envisioned sequence of events consists of erosion of a canyon into deformed vitrophyre and basalt layers. These eroded units were later covered by younger pyroclastic deposits while the eroded products were deposited a few hundred meters downstream by debris flow.

Vaguely bedded polylithologic breccia that locally overlies the debris-avalanche deposit between Cerro Pizarro and Cerro Las Animas represents reworking of the avalanche deposit by hyperconcentrated stream flow. The entire debris-avalanche succession, both mono-and polylithologic breccia, is overlain by the Zaragoza ignimbrite, which was derived from Los Humeros volcanic center 20 km to the north. The Zaragoza ignimbrite, in turn, is overlain by young pyroclastic material derived from Cerro Pizarro. The Zaragoza ignimbrite is dated at ~100 ka only by inference (Ferriz and Mahood 1984), but its presence in the section between debris-avalanche and young pyroclastic deposits indicates a significant hiatus.

Barranca S, on the southern flank of Cerro Pizarro, opens out from a narrow channel onto a broad plain. The fan-like outcrop morphology of young pyroclastic deposits on this plain suggests that the barranca was at least partially carved into the cone prior to the eruption and emplacement of these young deposits.

Late-stage growth of the present central edifice

The central part of Cerro Pizarro is conical in shape (Fig. 3), mimicking the dip of the surrounding, though lower elevation, ring. Some of this growth may have occurred during previous stages, but the form is not part of the collapse morphology, and so is assumed to post-date it. It seems unlikely, however, that endogenous growth in an unconfined space would produce the conical shape. Activity accompanying the growth of the central cone consisted of eruption of pyroclastic flows, falls, and surges, which deposited beds that mantle topography on the inner cone and across the debris apron (Figs. 5 and

8F). Flows lapped up against topography around the volcano and filled paleotopography, and pyroclastic deposits overlie the Zaragoza ignimbrite. Vitrophyre is ubiquitous in these younger deposits. Evidence for the derivation of this pyroclastic material from Cerro Pizarro comprises its radial distribution around the cone, the manner in which it drapes topography and clearly interacted with topography present at the time, and the lack of nearby silicic eruptive centers.

The contact of the highest and inferred youngest dome with older material is marked by the out-of-place succession of limestone conglomerate, pyroclastic rocks, and stony rhyolite breccia described above. This succession is inferred to represent the pre-dome facies-association deposits that are found vertically in Barranca S and horizontally in Barranca E, although basaltic strata are missing. Stony-rhyolite breccia may represent carapace deposits from the earliest dome. We infer that successive intrusions brought old strata upward along intrusive margins.

Discussion

The common perception of volcanic domes as relatively simple features derives in part from published descriptions (e.g., Christiansen and Lipman 1966; Metz and Bailey 1993; Duffield et al. 1995). In the generalized case, a stony interior is surrounded by a carapace of vitrophyre and breccia. Explosive units are generally confined to early stages of dome formation, and little modeling of controls on dome collapse has been done. In cases where multiple domes are superposed, the basic pattern is commonly repeated, yielding complex relations, but with a common theme of dome development. Understanding the potential of domes to behave in a very complex manner provides an important aspect to prediction and assessment of hazards related to these relatively small features.

Although the evolutionary stages of Cerro Pizarro shown individually can be compared to stages exhibited in common models of dome growth, its evolution as a whole can be envisaged as a unique system that was fundamentally far more complex than the more classic models predict. Little evidence remains at Cerro Pizarro for a "regular" succession of vent-clearing eruption followed by passive emplacement of an approximately mushroom-shaped edifice in which a brecciated, variably pumiceous and vitrophyric carapace surrounded a stony core. We speculate, however, that the earliest stage of dome formation did include a vent-clearing eruption (Fig. 8A), while the secondary phase approximately followed the more general pattern (Fig. 8B), largely owing to the preservation of a coherent, locally brecciated vitrophyre layer, in association with stony rhyolite. Other aspects of the early stages of Cerro Pizarro are certainly not contradicted by most models; the eruption of domes is well documented (Mount St. Helens, e.g., Rowley et al. 1981; Soufrière Hills Volcano, Montserrat, e.g., Cole et al. 1998; Young et al. 1998; Unzen, e.g., Sato et al. 1992; Nakada and Fujii 1993; Merapi, e.g., Andreastuti et al. 2000; Voight et al. 2000a).

Dome collapse is a common process at some erupting domes (Soufrière Hills, Merapi, Unzen); the observation of collapse events at these volcanoes has provided information about magma emplacement dynamics (e.g., Voight et al. 2000b; Watts et al. 2002). The major distinction in these cases is the size of the magmatic system—small dome systems clearly do collapse, even if they are rarely documented (e.g., Riggs et al. 1997). The majority of cases of collapse, however, is documented in domes associated with large stratovolcanoes like Citlaltépetl or Unzen or large dome complexes like Merapi.

In contrast, although the evolution of Cerro Pizarro is in part similar to that seen frequently at stratovolcanoes and in part similar to a cryptodome, the combination is far more complex than has been documented in isolated or clustered domes previously. In fact, Carrasco-Nuñez and Riggs (2002) recently compared the general evolution of Cerro Pizarro dome and Citlaltépetl stratovolcano and noted that overall, Cerro Pizarro followed the far more complex evolutionary path. Cryptodomal activity, as mentioned previously, is not uncommon in the geologic record, but has been recorded actively only at Showa Shinzan (Mimatsu 1995) and Mount St. Helens, the latter referring to the activity within the stratovolcano that led to collapse in 1980. At Cerro Pizarro, the cryptodome behaved in a manner similar to that of Mount St. Helens, deforming a relatively recent part of the volcano (although in a large stratovolcano, the locus of deformation may be fortuitous: the Showa Shinzan cryptodome grew on a distal flank of Mt. Usu). Likewise, how the host volcano reacted to the process of deformation is different: at Mount St. Helens, bowing caused cracking of surficial features and massive instability, which in turn led to collapse and blast that removed the great majority of the cryptodome; at Cerro Pizarro internal features were permanently deformed and apparently a relatively large proportion of the cryptodome was preserved in the central part of the dome system.

Hoblitt et al. (1981) speculated that the coherence of lava flows that make up the south flank of Mount St. Helens led to the localization of the cryptodome under the northern flank. At Cerro Pizarro, the approximate uniformity of deformed layers around the cone suggests that the cryptodome was emplaced more centrally. We speculate that in isolated cryptodomal systems, the volume of overlying material is insufficient to direct the migration of magma. In larger systems (i.e., Mount St. Helens, Showa-Shinzan), structural and lithologic variations act to focus magmatism into specific areas, in the same way that domes often grow in an irregular manner on stratovolcanoes.

At Cerro Pizarro the intrusion brought pre-existing units to vertical and near-vertical orientations. The final phase of cryptodome intrusion likely culminated with a explosive eruption directed to the west that caused the collapse of the western ring previously uplifted by the

initial injection of the cryptodome. Collapse caused minimal disruption of the already deformed strata, which were preserved surrounding the southern, eastern and northern flanks of Cerro Pizarro. This contrasts with Mount St. Helens, where sector collapse removed the traces of its origins.

Conclusions

In conclusion, we document here the evolution of a Pleistocene dome that went though six stages of eruption that cumulatively represent an evolutionary path previously undocumented in the growing literature on dome systems. The earliest stages are not dissimilar to more common models of dome evolution: the life of the dome began with probably localized vent-clearing eruptions that deposited breccia containing clasts of pre-volcanic bedrock, followed by likely explosive eruptions of dominantly ash and small fragments that were emplaced by surge, fall, and flow mechanisms concomitant with dome emplacement. This dome grew sufficiently to partially collapse, yielding block-and-ash-flow breccias. Renewed magma emplacement caused the formation of a cryptodome, which deformed surrounding older dome facies heterogeneously, in some places warping previously flat- or nearly flat-lying strata to vertical, and in others causing only minimal amounts of strain.

Sector collapse of the western quadrant of the cone was apparently caused by a combination of emplacement of fresh magma and potentially several earthquakes to cause instability in the volcano. The resultant debris avalanche traveled about 2 km to the west before encountering a bedrock ridge of Cretaceous limestone.

A major period of quiescence is indicated by the emplacement of the Zaragoza Ignimbrite, derived from Los Humeros volcanic center 20 km to the north, and by topography eroded into the volcano itself. Magma emplacement to create the final, present shape of the volcano was accompanied by numerous pyroclastic eruptions whose deposits drape both upper and fan parts of the volcano. Other thick breccias found around the volcano are assumed to represent the post-eruptive disintegration of the cone.

Small isolated domes clearly can evolve in the complex manner traditionally reserved for stratovolcano-system models. The cryptodomal stage, in particular, is probably far more common to domes than documented. The size of the cryptodome relative to the volcano suggests that in many cases, such a stage will not be recognized in a larger system.

Acknowledgements This work was partially supported by an AAAS/NSF Women's International Science Collaboration Program grant to NRR and Conacyt grant 27554-T and PAPIIT IN104401 to GCN. Thin sections were prepared by Juan Vazquez at UNAM. Aerial photographs were provided by Fidel Cedillo at Los Humeros Geothermal Field (CFE). Chemical analyses were performed at UNAM by Patricia Girón and Rufino Lozano. $^{40}Ar/^{39}Ar$ dating was done at the New Mexico Geochronological Research Lab by L. Peters and W.C. McIntosh. We are grateful to Siobhan McConnell for quality field assistance and to Wendell Duffield and Jocelyn McPhie for wading through an earlier version of this manuscript and substantially improving its content and organization. Reviews by Gill Norton and an anonymous reviewer are greatly appreciated. Continuous encouragement by Dante Morán, former director of Instituto de Geología at UNAM, is greatly appreciated.

References

Andreastuti SD, Alloway BV, Smith IEM (2000) A detailed tephrostratigraphic framework at Merapi Volcano, Central Java, Indonesia: Implications for eruption predictions and hazard assessment. J Volcanol Geotherm Res 100:51–67

Belousov A (1996) Deposits of the 30 March 1956 directed blast at Bezymianny Volcano, Kamchatka, Russia. Bull Volcanol 57:649–662

Carrasco-Núñez G (2000) Structure and proximal stratigraphy of Citlaltépetl Volcano (Pico de Orizaba), Mexico. In: Aguirre-Diaz G, Delgado-Granados H, Stock JM (eds) Cenozoic volcanism and tectonics of Mexico. Geol Soc Am Spec Pap 334:247–262

Carrasco-Núñez G, Gómez-Tuena A, Lozano VL (1997) Geologic map of Cerro Grande volcano and surrounding area, Central Mexico. Geol Soc Am Map and Chart Series MCH 081, 10 pp

Carrasco-Núñez G, Riggs NR (2002) Dome growth in monogenetic and polygenetic magmatic systems: Cerro Pizarro and Citlaltépetl volcanoes, eastern México. Mount Pelee 1902–2002. Explosive volcanism in subduction zones. Programe et resumes, p 18

Christiansen RL, Lipman PW (1966) Emplacement and thermal history of a rhyolite flow near Fortymile Canyon, southern Nevada. Bull Geol Soc Am 77:671–684

Cole PD, Calder ES, Druitt TH, Hoblitt R, Robertson R, Sparks RSJ, Young SR (1998) Pyroclastic flows generated by gravitational instability of the 1996–1997 lava dome of Soufriere Hills Volcano, Montserrat. Geophys Res Lett 25:3425–3428

Crandell DR, Miller CD, Glicken, HX, Christiansen, RL, Newhall CG (1984) Catastrophic debris avalanche from ancestral Mount Shasta Volcano, California. Geology 12:143–146

Crandell DR (1989) Gigantic debris avalanche of Pleistocene age fromancestral Mount Shasta Volcano, California, and debris-avalanche hazard zonation. US Geol Surv Bull B1861, 32 pp

Duffield WA, Jackson MD, Smith JG, Lowenstern JB, Clynne MA (1996) Structural doming over an upper crustal magma body at Alid, Eritrea. EOS Trans 77:792

Duffield WA, Richter DH, Priest SS (1995) Physical volcanology of silicic lava domes as exemplified by the Taylor Creek Rhyolite, Catron and Sierra Counties, New Mexico. US Geol Surv Map I-2399, 1:50,000

Ferriz H, Mahood GA (1984) Eruption rates and compositional trends at Los Humeros Volcanic Center, Puebla, Mexico. J Geophys Res 89:8511–8524

Fisher RV (1990) Transport and deposition of a pyroclastic surge across an area of high relief: the 18 May 1980 eruption of Mount St. Helens, Washington. Bull Geol Soc Am 102:1038–1054

Gómez-Tuena A, Carrasco-Núñez G. (2000) Cerro Grande volcano: The evolution of a Miocene stratocone in the early Trans-Mexican Volcanic Belt. Tectonophysics 318:249–280

Gorshkov GS (1959) The gigantic eruption of the volcano Bezymianny. Bull Volcanol 20:77–109

Hildreth W, Drake RE (1992) Volcán Quizapo, Chilean Andes. Bull Volcanol 54:93–125

Hoblitt RP, Miller CD, Vallance JW (1981) Origin and stratigraphy of the deposit produced by the May 18 directed blast. In: Lipman PW, Mullineaux DR (eds) The 1980 eruptions Mount St. Helens, Washington. US Geol Surv Prof Pap 1250:401–419

Ishikawa T (1950) New eruption of Usu Volcano, Hokkaido, Japan, during 1943–1945. J Fac Sci Hokkaido University 7:237–260

Kluth CF, Kluth MJ (1974) Geology of the Elden Mountain area, Arizona. In: Karlstrom TNV, Swann GA, and Eastwood RL (eds) Geology of northern Arizona with notes on archaeology and paleoclimate; Pt. II, area studies and field guides. Geol Soc Am Rocky Mtn Sec Mtg, Flagstaff, pp 521–529

Lipman PW, Moore JG, Swanson DA (1981) Bulging of the north flank before the May 18 eruption—geodetic data. In: Lipman, PW, Mullineaux DR (eds) The 1980 eruptions Mount St. Helens, Washington. US Geol Surv Prof Pap 1250:143–156

Lozano-Santa Cruz R, Verma SP, Girón P, Velasco F, Morán D, Viera F, Chávez G (1995) Calibración preliminar de fluorescencia de rayos-X para análisis cuantitativo de elementos mayores en rocas ígneas. Acta INAGEQ 1:203–208

Metz JM, Bailey RA (1993) Geologic map of Glass Mountain, Mono County, California. Misc Invest Ser US Geol Surv Report I–1995

Mimatsu M (1995) Showa-Shinzan Diary [English translation]. Executive Committee 50th anniversary of Mt. Showa-Shinzan, Hokkaido, Japan 179 pp

Minakami T, Ishikawa T, Yagi K (1951) The 1944 eruption of Volcano Usu in Hokkaido Japan. Bull Volcanol 11:45–160

Moore JG, Albee WC (1981) Topographic and structural changes, March–July 1980—photogrammetric data. In: Lipman PW, Mullineaux DR (eds) The 1980 eruptions Mount St. Helens, Washington. US Geol Surv Prof Pap 1250:123–134

Nakada S, Fujii T (1993) Preliminary report on the activity at Unzen Volcano (Japan), November 1990–November 1991: Dacite lava domes and pyroclastic flows. J Volcanol Geotherm Res 54:319–333

Riggs NR, Hurlbert JC, Schroeder TJ, Ward SA (1997) The interaction of volcanism and sedimentation in the proximal areas of a mid-Tertiary volcanic dome field, central Arizona, USA. J Sediment Res 67:142–153

Robinson HH (1913) The San Franciscan volcanic field, Arizona. US Geol Surv Prof Pap 76, 213 pp

Rosales-Hoz L, Santiago-Pérez S, Lozano-Santa Cruz R (1997) Modifications to a glass disk fusion method for X-ray fluorescence analyses of geological material. Acta INAGEQ 2:245–250

Rowley PD, Kuntz MA, MacLeod NS (1981) Pyroclastic-flow deposits. In: Lipman PW, Mullineaux DR (eds) The 1980 eruptions Mount St. Helens, Washington. US Geol Surv Prof Pap 1250:489–512

Sato H, Fujii T, Nakada S (1992) Crumbling of dacite dome lava and generation of pyroclastic flows at Unzen volcano. Nature 360:664–666

Siebe C (1985) Geologische, geochemische und petrographische Untersuchungen im Gebiet der rhyolithischen Dome Las Derrumbadas, Bundesstaat, Puebla, Mexiko. Diplomarbeit, Universität Tübingen, 97 pp

Siebert L (1984) Large volcanic debris avalanches: characteristics of source areas, deposits, and associated eruptions. J Volcanol Geotherm Res 22:163–197

Sparks RSJ, Barclay J, Calder ES, Herd RA, Komorowski J-C, Luckett R, Norton GE, Ritchie LJ, Voight B, Woods AW (2002) Generation of a debris avalanche and violent pyroclastic density current on 26 December (Boxing Day) 1997 at Soufrière Hills Volcano, Montserrat. In: Druitt TH, Kokelaar BP (eds) The eruption of Soufrière Hills Volcano, Montserrat, from 1995–1999. Geol Soc Lond Mem 21:409–434

Ui T (1983) Volcanic dry avalanche deposits—identification and comparison with nonvolcanic debris stream deposits. J Volcanol Geotherm Res 18:135–150

Ui T, Takarada S, Yoshimoto M (2001) Debris avalanches. In: Sigurdsson H (ed) Encyclopedia of volcanoes. Academic Press, San Diego, pp 617–626

Voight B, Glicken H, Janda RJ, Douglass PM (1981) The rockslide avalanche of May 18. In: Lipman PW, Mullineaux DR (eds) The 1980 eruptions Mount St. Helens, Washington. US Geol Surv Prof Pap 1250:347–377

Voight B, Constantine EK, Siswowidjoyo S, Torley R (2000a) Historical eruptions of Merapi Volcano, central Java, Indonesia, 1768–1998. J Volcanol Geotherm Res 100:69–138

Voight B, Komorowski JC, Norton GE, Belousov AB, Belousova M, Boudon G, Francis PW, Franz W, Heinrich P, Sparks RSJ, Young SR (2002c) The 26 December (Boxing Day) 1997 sector collapse and debris avalanche at Soufrière Hills Volcano, Montserrat. In: Druitt TH, Kokelaar BP (eds) The eruption of Soufrière Hills Volcano, Montserrat, from 1995–1999. Geol Soc Lond Mem 21:363–407

Voight B, Young KD, Hidayat D, Subandrio, Purbawinata MA, et al (2000b) Deformation and seismic precursors to dome-collapse and fountain-collapse nuées ardentes at Merapi Volcano, Java, Indonesia, 1994–1998. J Volcanol Geotherm Res 100:261–287

Watts RB, Herd RA, Sparks RSJ, Young SR (2002) Growth patterns and emplacement of the andesitic lava dome at Soufrière Hills Volcano, Montserrat. In: Druitt TH, Kokelaar PB (eds) The eruption of Soufrière Hills Volcano, Montserrat, from 1995 to 1999. Geol Soc Lond Mem 21 pp

Yáñez C, García S (1982) Exploración geotérmica de la región geotérmica Los Humeros-Las Derrumbadas, estados de Puebla y Veracruz. C.F.E. 96

Young SR, Sparks RSJ, Aspinall WP, Lynch LL, Miller AD, Robertson REA, Shepherd JB (1998) Overview of the eruption of Soufrière Hills Volcano, Montserrat, 18 July 1995 to December 1997. Geophys Res Lett 25:3389–3392